

## Characterization of different grades of aluminum anodes for aluminum/air batteries

M.L. Doche <sup>a,\*</sup>, F. Novel-Cattin <sup>b</sup>, R. Durand <sup>a</sup>, J.J. Rameau <sup>a</sup>

<sup>a</sup> *Laboratoire d'Electrochimie et de Physico-chimie des Materiaux et des Interfaces (U.M.R. No. 5631 C.N.R.S.), E.N.S.E.E.G./I.N.P.G., 38402 Saint Martin d'Hères, France*

<sup>b</sup> *Renault, Research Division, 9-11 Ave. du 18 juin 1940, 92500 Rueil-Malmaison, France*

Received 5 December 1996; accepted 7 December 1996

### Abstract

Aluminum/air batteries have received much attention during the last decade because of their possible application in the field of electric vehicle propulsion. Although this system presents good theoretical characteristics, its major problem is the low practical coulombic efficiency of aluminum in strong alkaline media, resulting from its high corrosion rate. Using a grade of high purity aluminum helps to reduce corrosion but increases the material cost. Moreover, aluminum dissolves while discharging the battery, leading to an enrichment of the electrolyte in soluble aluminate species, which has a detrimental effect on the cell performance, so the electrolyte should be continuously treated by the means of a crystallizer coupled to the battery. In this context, the aim of the study is to find experimental conditions which could permit the use of a lower-cost grade of aluminum with respect to the cell and regenerator performances.

**Keywords:** Aluminum anode primary batteries; Aluminum; Applications/electric vehicles

### 1. Introduction

The small number of electric vehicles inhibits drastically the development of their market. One way to improve this situation is to power the cars with generators such as fuel cells or metal/air batteries which have energy densities many times greater than conventional secondary batteries [1]. Amongst the numerous metal/air systems, the aluminum/air technology has an excellent theoretical energy density (8.1 kWh kg<sup>-1</sup> of aluminum) combined with a high theoretical cell voltage of 2.71 [2]. Further arguments for its consideration are the rather low production cost of aluminum and the existence of a large base for its manufacture and distribution.

Most of the aluminum/air batteries developed during the past decade work with strongly alkaline electrolyte (KOH or NaOH), permitting optimal performances of the air cathode [3], as well as a low level of aluminum polarization during normal operation. However, aluminum suffers substantial corrosion in alkaline solution, which induces coulombic loss on discharge and fuel loss during standby.

To overcome this problem, many researchers have used aluminum alloys of high purity grades possibly doped with elements like Ga, In, Sn, Mg, Mn, Tl [4–8], which act as

corrosion inhibitors without increasing the overvoltage for aluminum dissolution.

The main aspect of alloy preparation is to use a high purity aluminum base, not less than 5N (99.999% purity), because iron impurities, normally present in a raw cast aluminum, drastically increase its corrosion rate [6,9,10]. However, the high cost in energy of such a grade (40 kWh kg<sup>-1</sup>) reduces the overall thermodynamic efficiency of the battery (also taking into account the faradic efficiency and the overpotential of both anodic and cathodic reactions) to close to 10%. Moreover, its production price, 10 to 20 times greater than the industrial 2N7 aluminum, does not satisfy the requirements for commercial application.

The possible integration of the aluminum/air cell in an electric vehicle also made us consider the industrial regeneration of alumina (the crystallized oxidation product) into aluminum metal. The KOH electrolyte usually used in an aluminum/air battery does not allow the retreatment of alumina via the industrial Hall–Heroult process, because potassium ions have harmful effects on the cathode of the electrolysis cell [11]. Consequently, all the experiments were carried out with sodium hydroxide electrolytes.

The aim of our study was to analyze the feasibility of using a lower grade (and hence lower priced) aluminum as anode material in the battery. For this purpose, we tried to determine

\* Corresponding author.

cell working conditions, such as temperature, NaOH concentration, and corrosion inhibitor level, allowing the use of less pure aluminum without excessively affecting the cell performances, in terms of polarization and corrosion resistance.

Effects of the concentration of the aluminum dissolution product (aluminates) were also tested to evaluate the necessity of a continuous regeneration of the electrolyte. Measurements of aluminum characteristics were performed on a pilot scale (minimum anode area: 100 cm<sup>2</sup>) using an Alupower-Chloride aluminum/air cell, in order to extrapolate as accurately as possible the real performances that could be reached in a full scale battery.

## 2. Experimental

### 2.1. Experimental test assembly

Preliminary studies were conducted on a 3 kW aluminum/air battery supplied by Alupower-Chloride and composed of 48 cells. Each cell of the stack was made of two air cathodes mounted on a plastic support to form the cathodic envelope. The air cathodes were of type AE-100, manufactured by ELTECH and remained unchanged throughout all the experiments. They were supplied with untreated room air.

The aluminum anode, a single plate of 175 cm<sup>2</sup> of working surface (dimensions 170 mm long, 100 mm wide and 12 mm thick), is inserted into the cathodic envelope so that each of its two main faces are located in front of the corresponding cathode. The overall cell surface is then 350 cm<sup>2</sup> and the distance between the anodic and cathodic surfaces is around 2 mm.

To study the anode performances when discharging in the cell, we made an experimental test assembly which allowed us to control the temperature and electrolyte flow rate. A diagram of the test assembly is shown in Fig. 1.

This is composed of three main elements:

- (i) the power module which is the cell itself;
- (ii) the service block: including an electrolyte storage tank and a circulation loop for the electrolyte (and possibly water as a circuit cleaning system);
- (iii) the monitoring and control unit permitting the definition of discharge conditions to measure cell performances.

### 2.2. Introduction of a reference electrode within the cell

Monitoring the anode potential needs accurate measurements. For this purpose we designed a special system to introduce a reference electrode inside the small gap between anode and cathode, and to keep it as close as possible to the anode surface, so minimizing the *IR* drop.

This system consists of an Hg/HgO reference electrode immersed in 1 M NaOH, so as to protect its glass body from attack by hot concentrated alkaline solution and maintain its potential independent of concentration and temperature conditions within the cell ( $E_{\text{Hg/HgO}} = 0.9267$  V versus RHE  $\approx 0.1$  V versus SHE [12]). The reference compartment was connected to a very thin capillary ( $\phi_{\text{int}} = 0.13$  mm), covered by a PTFE protecting film, via a PTFE capillary. The capillary was mounted on a special support which also acted as a lid for the cell. The support was used to direct the thin capillary toward the aluminum surface (see Fig. 2). Because special attention was focussed on the reliability of the potential meas-

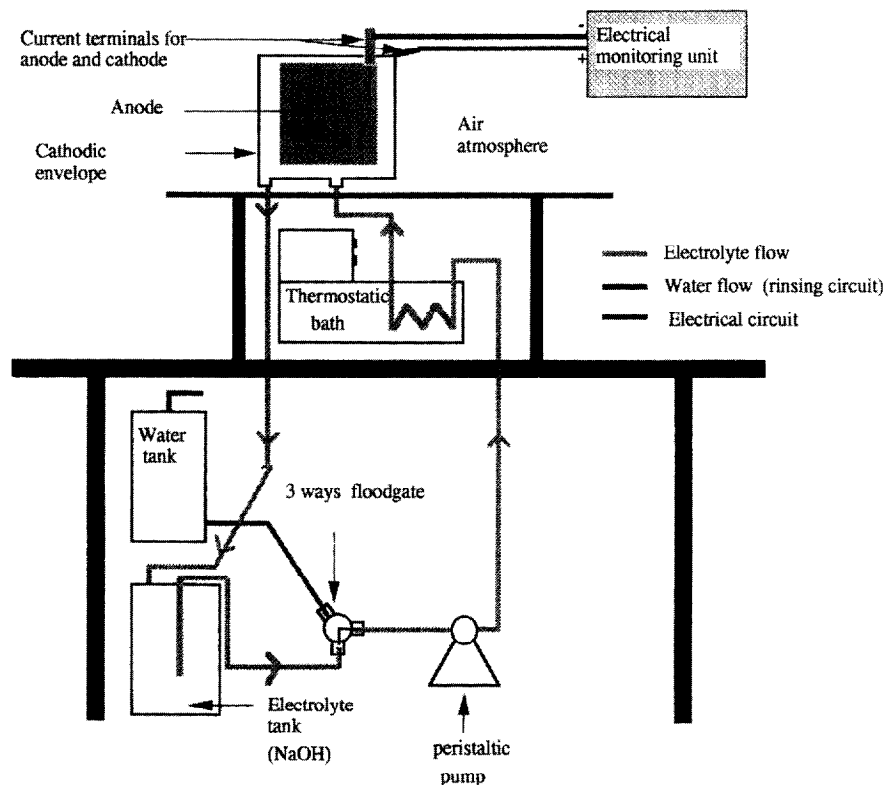


Fig. 1. Schematic of the aluminum/air test rig.

measurements, two reference electrodes were introduced into the cell, one either side of the anode.

### 2.3. Electrical monitoring unit for the cell

Measurements of the anodic potential versus cell current could normally be achieved by using a triple-input potentiostat. According to the electrode surfaces, the current output from the cell can often reach 60 A at a cell voltage of 1 V. The prohibitive cost of a 100 A potentiostat obliged us to create a regulation device which allowed us to work under constant current density or constant potential conditions and to plot polarization curves.

The cell control and monitoring system is presented in Fig. 2. It was composed of:

- (i) an electric load (type CMPR 4004) which permitted the monitoring of the cell discharge current;
- (ii) a Fluke voltmeter ( $Z=1$  Mohm) for the cell voltage measurement;
- (iii) two high input impedance voltmeters ( $Z \geq 1$  Gohm), from Keithley and Tacussel, used to measure the anodic potential;
- (iv) an HP microcomputer which controlled all devices.

We elaborated on three regulation softwares to permit the simulation of the potentiostat functions.

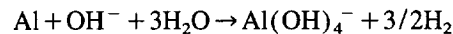
(a) Potentiostatic measurements were achieved using a software based on simplified PID regulation. The principle of the method was to choose a level of anodic potential and to monitor the cell current in such a way that the anodic potential measured became close to this, with an accuracy of 5 mV.

(b) Constant current experiments used a different regulation procedure. The load is able to fix a constant current between the two terminals of the cell and we can measure the potential evolution as a function of time.

(c) Polarization curves were plotted point by point, using the constant current control method. However, hydrogen evolved on the anodic surface was able to generate instability in the measurement of potential and it was necessary to ensure that each point of the curve was obtained under steady state conditions. To rapidly determine the average steady state potential, a numeric filter was added to the regulation program.

### 2.4. Measurement techniques

In alkaline media, aluminum is corroded by water according to the reaction:



We used a steady state potentiostatic technique to determine the partial current of hydrogen evolution and aluminum oxidation, as a function of the anodic potential. As the anodic potential was held constant, the electrode current was recorded for at least 30 min until steady state conditions were reached. The mean corrosion current was determined by weight loss between the beginning and the end of the experiment and converted to an equivalent current using Faraday's law. To increase the accuracy of the measurements, 350 cm<sup>2</sup> anodes were used.

However, the maximum current output from the cell, was limited to 60 A (170 mA cm<sup>-2</sup>), because the load cannot apply a current at cell voltages lower than 1 V. Such a cell voltage is commonly reached for a current = 60 A, because of the high polarization of the air cathodes. Because of this load functioning limitation, polarization curves were performed on a smaller anodic surface (100 cm<sup>2</sup>) in order to explore a larger range of anodic potentials. Double scan polarization curves were recorded including direct (increasing potential direction) and reverse scans.

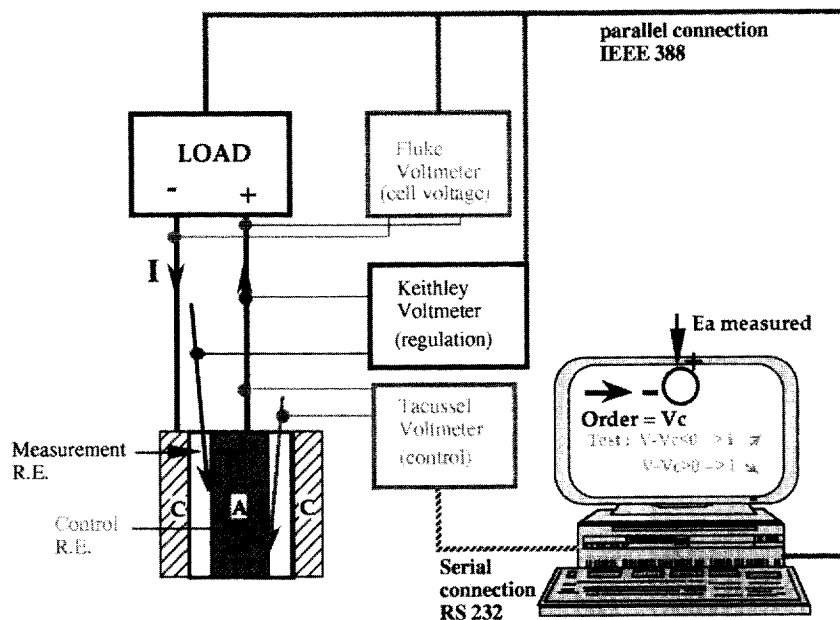


Fig. 2. Diagram of the electrical monitoring unit.

Before each experiment, we also proceeded to a 'surface stripping' treatment of the anode which consists of a constant current oxidation ( $i = 200 \text{ mA cm}^{-2}$ ), lasting 15 min. This treatment is done to dissolve the alumina layer formed by air oxidation and so ensure an initially homogenous anodic surface state, reproducible from one experiment to another.

### 2.5. Experimental conditions

During this study, four aluminum alloys were tested. The first one, produced by ALCAN, is made of 99.999% pure aluminum doped with 0.1 wt.% of tin and 0.5 wt.% of magnesium.

Its composition has been optimized for use in the Alupower battery [13] under nominal conditions specified by the manufacturer: electrolyte: 8 M KOH; temperature: 60°C; use of sodium stannate as corrosion inhibitor in the electrolyte: 0.01 M.

In order to decrease the anodic cost, we also selected three grades of unalloyed aluminium:

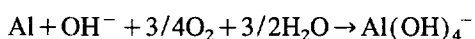
- 2N7 commercial grade (99.7% purity, 15 kWh kg<sup>-1</sup>),
- 3N5 grade (pure at 99.95%, 20 kWh kg<sup>-1</sup>) which has been refined in order to decrease its Fe content below 10 ppm,
- 5N grade (pure at 99.999%, 35 kWh kg<sup>-1</sup>) obtained by an electrorefining process.

Standard electrochemical conditions were settled according to the battery suppliers specifications and with respect to the aim of our study.

The electrolyte temperature was around  $60 \pm 5^\circ\text{C}$ , being a value advised by Alupower.

The electrolyte used was NaOH in a range of concentrations around  $4 \text{ M} \pm 1 \text{ M}$ . According to the solubility of aluminate ions in sodium hydroxide [14], working with higher NaOH concentrations would not permit the precipitation of  $\text{Al}(\text{OH})_4^-$  into  $\text{Al}(\text{OH})_3$  in the regenerator.

The effect of aluminate concentration on the cell performances was studied in the range  $0\text{--}20 \text{ g l}^{-1}$ , corresponding to 70% of their maximum solubility in 4 M NaOH at 60°C. Solutions containing aluminate ions were prepared by electrochemical dissolution of 5N aluminum in the cell. The initial NaOH concentration of the solution was calculated so as to obtain a 4 M concentration after dissolution of  $x \text{ M}$  aluminum, with respect to the stoichiometry of the overall cell reaction:



The corrosion inhibitor used was sodium stannate. We explored a range of concentrations ( $0.05 \text{ M} \pm 0.03 \text{ M}$ ) — slightly higher than Alupower's standard conditions — to make the use of lower purity aluminum grades possible.

## 3. Results

### 3.1. Preliminary experiments

Before studying the different aluminum grades, we performed preliminary experiments in order to test the system

stability as well as the reliability of potential measurements. The stability of the potential measurements depends on the corrosion rate, because hydrogen bubbles generated on the anode surface induce a variable ohmic drop between the reference capillary extremity and the anodic interface. As the aluminum corrosion rate also depends on the anodic polarization, it was measured, as a function of time, for two applied current values, respectively, 10 and 20 A (100 and 200 mA cm<sup>-2</sup>).

The influence of the electrolyte flow rate was also evaluated, in the range  $0.8\text{--}1.8 \text{ l min}^{-1}$ , because hydrodynamic conditions are liable to modify the aluminum dissolution rate, and to facilitate the evacuation of hydrogen bubbles. Experiments were done on the 3N5 grade (supposed to be more sensitive to corrosion) in 4 M NaOH solutions containing 0.05 M sodium stannate, at 60°C. Each experiment was reproduced twice. Potential–time curves are presented in Fig. 3.

The standard deviation of potential as a function of time is around 5 mV for measurements performed at 10 A, and 10 mV at 20 A. Potential variations are proportional to the applied current, indicating that they are due to the ohmic drop between the reference capillary and the anode surface. It also means that temporary changes of electrolyte resistivity, due to hydrogen bubbles, are of similar orders of magnitude for the two explored current densities.

Fig. 3 also shows that steady state conditions are obtained after only 5 min. The anode potential is independent of the electrolyte flow rate, whatever the applied current, and the replicate standard deviation at constant current does not exceed 5 mV. By these tests, we have validated the reference systems used for potential measurements. In the rest of the study, the flow rate was kept at  $0.8 \text{ l min}^{-1}$  to avoid any risk of electrolyte overflowing.

### 3.2. Comparative performances of the four aluminum alloys

The ALCAN alloy and the three grades of unalloyed metal were characterized at 60°C in 4 M NaOH containing 0.05 M  $\text{Na}_2\text{SnO}_3$  and  $20 \text{ g l}^{-1} \text{ Al}(\text{OH})_4^-$ . For each of the four, we have recorded potential–time values during surface stripping treatment at  $i = 200 \text{ mA cm}^{-2}$ , and we have plotted polarization curves. Each experiment was again reproduced three times to ensure the reliability of the results.

Concerning the 2N7 grade, it was not possible to measure its electrochemical characteristics because of the extremely high corrosion rate which disrupts potential measurements. We consider that it cannot be used as an anode for an aluminum/air cell.

Fig. 4 shows a comparison of the average polarization performances obtained by constant current measurements and by polarization curves.

According to Fig. 4(a), it takes a longer time for the ALCAN alloy to reach steady state compared to unalloyed grades. This might be due to the initial surface enrichment of alloying elements [8]. Nevertheless, its steady state potential

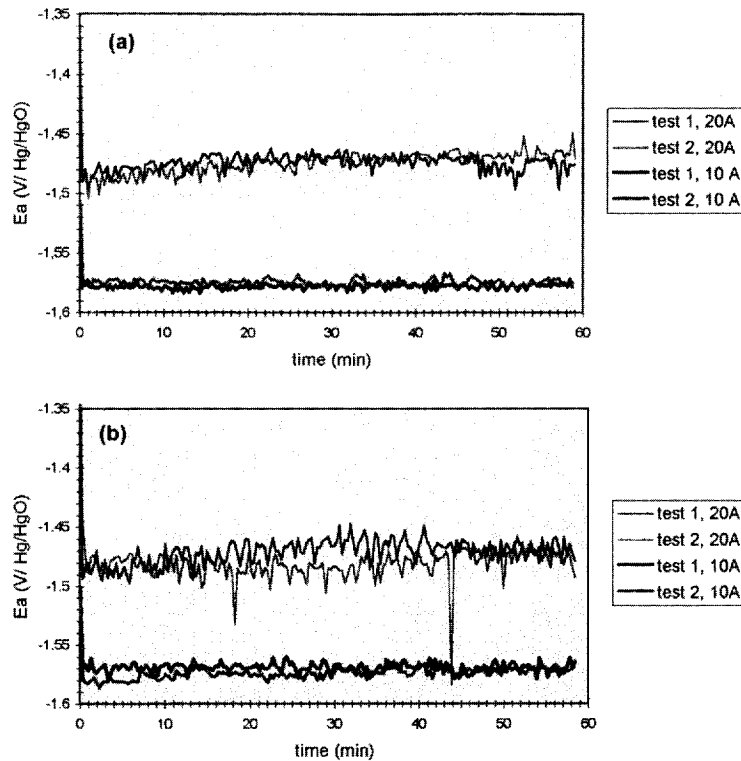


Fig. 3. Potential–time graphs for aluminum 3N5.  $i = 100 \text{ mA cm}^{-2}$  (10 A) and  $200 \text{ mA cm}^{-2}$  (20 A). In 4 M NaOH + 0.05 M  $\text{Na}_2\text{SnO}_3$  at  $60^\circ\text{C}$ . Electrolyte flow rates: (a)  $0.8$ ; (b)  $1.8 \text{ l min}^{-1}$ .

value at  $i = 200 \text{ mA cm}^{-2}$ , differs by only 20 mV from that of the 3N5 and 5N grades. According to the polarization curves, Fig. 4(b), it appears that the ALCAN alloy exhibits a more negative open circuit potential ( $E_a = -1.870 \text{ V}$  versus Hg/HgO instead of  $-1.8 \text{ V}$  versus Hg/HgO for the 5N grade) and a greater dissolution rate in the potential range from  $-1.870$  to  $-1.6 \text{ V}$  versus Hg/HgO, than unalloyed grades. For higher anodic potentials, the three electrodes behave very similarly. The overpotential of the 3N5 grade is only 20 mV greater than that of the super pure 5N throughout the range of explored potential.

Corrosion characteristics of each alloy were also measured in similar working conditions, for  $I = 0 \text{ A}$  and  $E_a = -1.65 \text{ V}$  versus Hg/HgO. Results are summarized in Table 1.

All three alloys undergo substantial corrosion under open circuit conditions. The 3N5 exhibits a corrosion rate 10% higher than the 5N and 24% higher than the ALCAN, meaning that the presence of impurities in the aluminum has a detrimental effect upon its corrosion characteristics. Under discharge conditions ( $E_a = -1.65 \text{ V}$  versus Hg/HgO), the

corrosion current is clearly reduced, leading to coulombic efficiencies ( $\rho_{\text{coul}} = i / (i + i_{\text{corr}})$ ) of 96.8, 95.6 and 91.2%, respectively, for the ALCAN, 5N and 3N5.

Discharge characteristics of the 3N5 grade are however acceptable. Its dissolution rate is almost identical to those of the 5N grade and its coulombic efficiency might be increased when working at higher current density. To confirm this fact, we have plotted a delineated polarization curve on this grade, showing the overall current density and the partial current densities for hydrogen evolution and aluminum oxidation. Measurements were performed at  $60^\circ\text{C}$ , in 4 M NaOH containing 0.05 M  $\text{Na}_2\text{SnO}_3$  but no aluminates. Fig. 5 shows a comparison between values obtained with and without aluminate. Some of the results are summarized in Table 2.

From these results, it appears that aluminate products contribute to a decrease in the aluminum dissolution rate as well as in the kinetics for  $\text{H}_2$  evolution. In aluminate-free NaOH solution, the 3N5 grade exhibits a lower overpotential under constant applied current, but also a corrosion rate which is drastically increased. The coulombic efficiency at  $-1.65 \text{ V}$

Table 1

Corrosion characteristics of the ALCAN, 5N and 3N5 alloys at  $i = 0$  and  $E_a = -1.65 \text{ V}$  versus Hg/HgO. In 4 M NaOH at  $T = 60^\circ\text{C}$ , containing 0.05 M  $\text{Na}_2\text{SnO}_3$  and  $20 \text{ g l}^{-1} \text{ Al}(\text{OH})_4^-$

		ALCAN	5N	3N5
$I = 0 \text{ A}$	$E_a$ (V vs. Hg/HgO)	-1.87	-1.79	-1.78
	$i_{\text{corr}}$ ( $\text{mA cm}^{-2}$ )	12.1	13.5	15
$E_a = -1.65 \text{ V vs. Hg/HgO}$	$i$ ( $\text{mA cm}^{-2}$ )	75	65	55
	$i_{\text{corr}}$ ( $\text{mA cm}^{-2}$ )	2.4	3	5.3

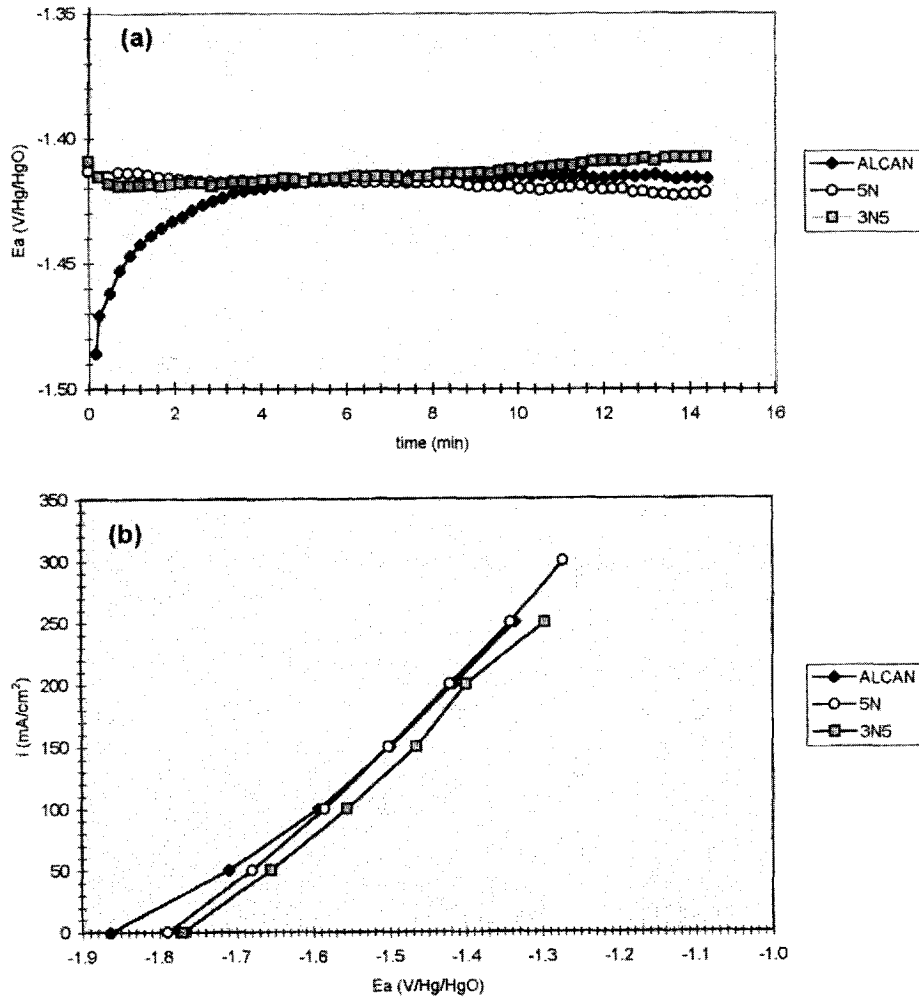


Fig. 4. Polarization characteristics obtained from ALCAN, 5N and 3N5 alloys in 4 M NaOH + 0.05 M Na<sub>2</sub>SnO<sub>3</sub> + 20 g l<sup>-1</sup> Al(OH)<sub>4</sub><sup>-</sup> at 60°C: (a) potential–time behavior under  $i = 200 \text{ mA cm}^{-2}$ ; (b) polarization curves.

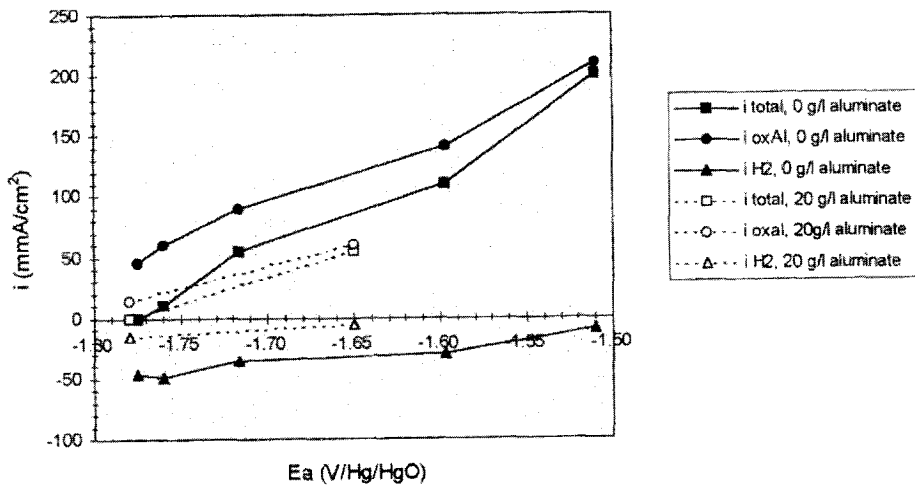


Fig. 5. Polarization curves obtained from aluminum 3N5 at 60°C in 4 M NaOH + 0.05 M Na<sub>2</sub>SnO<sub>3</sub> with 0 or 20 g l<sup>-1</sup> Al(OH)<sub>4</sub><sup>-</sup>.

versus Hg/HgO is 71.3% which is a lot smaller than the value (91.2%) obtained at the same potential in electrolyte containing aluminate. Extrapolation of the results recorded in aluminate-containing solutions (Fig. 5) permits us to think that the corrosion current at  $i = 200 \text{ mA cm}^{-2}$ , would be around  $1 \text{ mA cm}^{-2}$  for an anodic potential of  $-1.410 \text{ V}$

versus Hg/HgO (Fig. 4). Optimization of the cell working conditions should maximize the coulombic efficiency of the anode and minimize its overpotential.

Normal cell conditions necessitate working at current densities close to  $200 \text{ mA cm}^{-2}$ . For such polarization, the coulombic efficiency is greater than 95% whatever the aluminate

Table 2

Corrosion characteristics of alloy 3N5 in 4 M NaOH + 0.05 M Na<sub>2</sub>SnO<sub>3</sub> at 60°C and containing 0 or 20 g l<sup>-1</sup> aluminate ions

		3N5 grade in 4 M NaOH, T=60°C,  Na <sub>2</sub> SnO <sub>3</sub>   = 0.05 M	
		Al(OH) <sub>4</sub> <sup>-</sup>   = 0 g l <sup>-1</sup>	Al(OH) <sub>4</sub> <sup>-</sup>   = 20 g l <sup>-1</sup>
I = 0 A	E <sub>a</sub> (V vs. Hg/HgO)	-1.775	-1.78
	i <sub>corr</sub> (mA cm <sup>-2</sup> )	46.4	15
E <sub>a</sub> = -1.65 V vs. Hg/HgO	i (mA cm <sup>-2</sup> )	87	55
	i <sub>corr</sub> (mA cm <sup>-2</sup> )	35	5.3
E <sub>a</sub> = -1.5 V vs. Hg/HgO	i (mA cm <sup>-2</sup> )	200	138
	i <sub>corr</sub> (mA cm <sup>-2</sup> )	10	

content. The performance limitation is due to the overpotential E<sub>a</sub>(i) - E<sub>th</sub>, where E<sub>a</sub>(i) is the anode potential when polarized at a current density i, E<sub>th</sub> is the thermodynamic potential of the electrode, depending on the electrolyte pH and aluminate content (E° Al/Al(OH)<sub>4</sub><sup>-</sup> = -2.31 V versus ENH, corresponding to -2.41 V versus Hg/HgO [15]).

Anode overpotentials at i = 200 mA cm<sup>-2</sup> were found to be respectively 0.91 and 1 V for aluminate free and aluminate containing solutions, giving a significant decrease in the overall cell performances. Increasing the dissolution rate of the alloys would then allow a substantial decrease in the anode overpotential.

3.3. Optimization of the discharge behavior of 3N5, the lower purity grade of alloy

Further investigations were then carried out on the 3N5 grade with the aim of finding those working conditions that would allow us to minimize its polarization under i = 200 mA cm<sup>-2</sup>.

As aluminates are necessarily produced during normal cell operation, their concentration was maintained to a constant value of 20 g l<sup>-1</sup> in the electrolyte. Experiments were performed to analyze the influence of working conditions such as NaOH concentration, temperature and stannate concentration on the anodic potential. For this purpose, we used the methodology of experimental design, in order to model the response (E<sub>a</sub> under i = 200 mA cm<sup>-2</sup>) as a function of the studied parameters and to find a set of optimal conditions.

The working conditions were explored in the range:

- electrolyte, NaOH: 3–5 M
- corrosion inhibitors, Na<sub>2</sub>SnO<sub>3</sub>: 0.02–0.08 M
- temperature: 55–65°C

Table 3

Matrix of experiments

Experiment	I	NaOH	Stannate	Temperature
1	1	-1	-1	-1
2	1	-1	-1	1
3	1	-1	1	-1
4	1	-1	1	1
5	1	1	-1	-1
6	1	1	-1	1
7	1	1	1	-1
8	1	1	1	1

Each parameter is a reduced and centered variable setting the lower limit of the variation interval as -1, and the upper limit as +1.

The matrix of experiments was built using a full 2<sup>3</sup> design with eight experiments (see Table 3 for the matrix). This number is related to the three parameters studied each having 2 levels, -1 or +1. Using such a matrix, we propose to give a linear model of the response, including coefficients related to the interaction between parameters.

The model equation is:

$$E_a = a_0 + a_1X_{NaOH} + a_2X_{Na_2SnO_3} + a_3X_T + a_{12}X_{NaOH \times Na_2SnO_3} + a_{13}X_{NaOH \times T} + a_{23}X_{Na_2SnO_3 \times T}$$

with: X<sub>NaOH</sub> = (|NaOH| - 4)/1, X<sub>Na<sub>2</sub>SnO<sub>3</sub></sub> = (|Na<sub>2</sub>SnO<sub>3</sub>| - 0.05)/0.03, X<sub>T</sub> = (T - 60)/5.

Each experiment was repeated twice, in order to evaluate the replicate standard deviation. The statistical resolution of this design was realized thanks to the ECHIP® software [16] which calculates each coefficient and is able to fit the optimal model. The statistical criterion used to decide on the best model is based on the comparison between the residual standard deviation (RES SD) of the model and the replicate standard deviation (REP SD). Their ratio should be close to 1. ECHIP® also associates a square correlation coefficient with the model:

R<sup>2</sup> = 1 - [(RES SD)<sup>2</sup>/Σ(E<sub>a</sub>(i) - E<sub>ai</sub>)<sup>2</sup>], which should also be close to one when the model correctly fits the measurements. The results are presented in the matrix of Table 4.

After calculation, all coefficients were found to have a significant influence on the response, so that the best model (R<sup>2</sup> = 0.98) for E<sub>a</sub> at i = 200 mA cm<sup>-2</sup> was calculated to be:

$$E_a \text{ (mV)} = -1406 + 15.7 \times (|\text{NaOH}| - 4) + 8.9 \times (|\text{Na}_2\text{SnO}_3| - 0.05) / 0.03 - 23.8 \times (T - 60) / 5 - 2.7 \times (|\text{NaOH}| - 4) \times (|\text{Na}_2\text{SnO}_3| - 0.05) / 0.03 - 8.2 \times (|\text{NaOH}| - 4) \times (T - 60) / 5 + 5.6 \times (|\text{Na}_2\text{SnO}_3| - 0.05) / 0.03 \times (T - 60) / 5$$

The average value given by the model (E<sub>a</sub> = -1.406 V versus Hg/HgO) is in agreement with previous results giving E<sub>a</sub> = -1.410 mV versus Hg/HgO. From this result, it appears

Table 4  
Experimental results obtained by using the matrix

Test	$I$	$ \text{NaOH} $	$ \text{Na}_2\text{SnO}_3 $	$T$	$ \text{NaOH} $ $\times  \text{Na}_2\text{SnO}_3 $	$ \text{NaOH} $ $\times T$	$ \text{Na}_2\text{SnO}_3 $ $\times T$	$E_{a1}$ (V vs. Hg/HgO)	$E_{a2}$ (V vs. Hg/HgO)
1	1	-1	-1	-1	1	1	1	-1.419	-1.410
2	1	-1	-1	1	1	-1	-1	-1.453	-1.451
3	1	-1	1	-1	-1	1	-1	-1.400	-1.395
4	1	-1	1	1	-1	-1	1	-1.420	-1.425
5	1	1	-1	-1	-1	-1	1	-1.360	-1.353
6	1	1	-1	1	-1	1	-1	-1.443	-1.430
7	1	1	1	-1	1	-1	-1	-1.365	-1.355
8	1	1	1	1	1	1	1	-1.406	-1.410
Coefficient	$a_0$	$a_1$	$a_2$	$a_3$	$a_{12}$	$a_{13}$	$a_{23}$		

that an electrolyte concentration higher than 4 M significantly increases the anode polarization. This might be due to the fact that higher hydroxyl ion concentration also contributes to an increase in the corrosion rate. From this point of view, using a 3 M NaOH electrolyte would also improve the coulombic efficiency. Moreover, low NaOH concentration is preferable when coupling of the cell to an electrolyte regenerator. The experiments showed that temperature increases the dissolution rate of aluminum. More surprising is the effect of the stannate concentration, which seems to increase  $E_a$  when present at a concentration higher than 0.05 M. This indicates that too much inhibitor tends to slow the kinetics for aluminum oxidation.

However, working at a lower inhibitor concentration might have a harmful effect on the coulombic efficiency. It is therefore preferential to choose a stannate concentration slightly lower than 0.05 M. Optimal working conditions were therefore chosen as follows:

temperature: 65°C

$|\text{NaOH}| = 3 \text{ M}$

$|\text{Na}_2\text{SnO}_3| = 0.04 \text{ M}$

This leads to an optimum potential value of  $-1.460 \text{ V}$  versus Hg/HgO.

The coulombic efficiency of such a condition was not evaluated but might be greater than 95%. The potential difference  $E_a - E_{th}$  is decreased to 0.95 V. The potential gain is all the more important when considering a cell stack. For a 10 kW battery, corresponding to an assembly of 143 cells (1 V, 70 A), a gain of 50 mV of anodic polarization would increase the power by 500 W (5%).

#### 4. Conclusions

During this study, an experimental assembly was designed which permitted us to test aluminum/air cells with electrode surface areas of 350 cm<sup>2</sup> on a pilot scale.

We have made a special reference electrode system in order to record the anodic potential during discharge. In spite of small perturbations of the potential measurements, due to

hydrogen evolution at the anode surface, preliminary studies have shown a good reproductibility of the results.

Using custom-designed software for the regulation of experiments, we have characterized the electrochemical behavior of three aluminum alloys (ALCAN 0.1% Sn–0.5% Mg; aluminum 5N; aluminum 3N5), under constant applied current or potential, and by steady state polarization curves. The aim of this study was to make possible the use of the lower purity grade aluminum (3N5) in the cell, with performances comparable to that of super-pure aluminum. Experiments were done in 4 M NaOH solutions at 60°C and containing 0.05 M of corrosion inhibitors ( $\text{Na}_2\text{SnO}_3$ ) and  $20 \text{ g l}^{-1} \text{ Al}(\text{OH})_4^-$ .

The 3N5 aluminum anodes were found to exhibit similar polarization performances to those of other alloys, but suffered from a higher corrosion rate. Coulombic efficiency was 91.2% at  $i = 50 \text{ mA cm}^{-2}$  ( $E_a = -1.65 \text{ V}$  versus Hg/HgO) but might be greater than 95% under  $i = 200 \text{ mA cm}^{-2}$  ( $E_a = -1.410 \text{ V}$  versus Hg/HgO). In aluminate-free solutions, the kinetics for aluminum dissolution are enhanced but the anode undergoes a higher corrosion rate.

Polarization performances of this alloy were then studied in a different range of working parameters, with the aim of finding optimal conditions, which would permit a decrease of the anodic potential at  $i = 200 \text{ mA cm}^{-2}$ . The best set of parameters was found to be NaOH 3 M,  $T = 65^\circ\text{C}$ ,  $|\text{Na}_2\text{SnO}_3| = 0.04 \text{ M}$ , leading to an anodic potential of  $-1.460 \text{ V}$  versus Hg/HgO, i.e. 50 mV lower than in previous conditions.

More fundamental studies are under development to explain the influence of stannate and aluminate contents on the anodic behavior of aluminum in concentrated NaOH solutions [17].

#### References

- [1] D. Linden (ed.), *Handbook of Batteries*, McGraw-Hill, New York, 2nd edn., 1995.
- [2] G. Scamans, Development of the aluminium/air battery, *Proc. Meet. Electrochemical Technology Group of the SCI, London, Oct. 1985*.



- [3] D.D. MacDonald and C. English, *J. Appl. Electrochem.*, 20 (1991) 405.
- [4] D.D. MacDonald, K.H. Lee, A. Moccari and D. Harrington, *Corrosion Sci.*, 44 (1988) 652.
- [5] D.D. MacDonald, S. Real and M. Urquidi-MacDonald, *J. Electrochem. Soc.*, 135 (1988) 1397.
- [6] J. Hunter, The anodic behaviour of aluminium alloys in alkaline solution, *Thesis Rep.*, Oxford University, 1989.
- [7] C.D.S. Tuck, J.A. Hunter and G.M. Scamans, *J. Electrochem. Soc.*, 134 (1987) 2970.
- [8] K. Nisancioglu and L. Odden (eds.), *2nd Symp. Electrode Materials and Processes for Energy Conversion and Storage*, Vol. 87-12, The Electrochemical Society, Pennington, NJ, 1987, p. 499.
- [9] W. Schneider and K. Wiesener, *Bull. Soc. Chim. Beograd*, 48 (1983) 241.
- [10] J. Albert, M. Anbu Kulandainathan, M. Ganesan and V. Kapai, *J. Appl. Electrochem.*, 19 (1989) 547.
- [11] K. Grjotheim and B.J. Welch, *Aluminium Smelter Technology*, Aluminium-Verlag, Düsseldorf, 2nd edn., 1988, p. 52.
- [12] J. Balej, *Int. J. Hydrogen Energy*, 10 (1985) 365.
- [13] S. Lapp, 3 kW net power aluminium/air battery: system verification and performance, *Internal Rep. No. 076-700-001*, Alupower, 1992, pp. 1–15.
- [14] C. Misra, *Chem. Ind.*, (May) (1970) 619.
- [15] A.J. Bard, R. Parsons and J. Jordan, *Standard Potentials in Aqueous Solution*, Marcel Decker, New York, 1985.
- [16] ECHIP®, Version 6.1.0, Bob Wheeler, Pentium Safe.
- [17] M.L. Doche, R. Durand and J.J. Rameau, Electrochemical behaviour of aluminium in concentrated NaOH solutions, Oct. 1996, submitted for publication.